

## COSY-JÜLICH A SYNCHROTRON AND STORAGE RING FOR MEDIUM ENERGY PHYSICS

R. Maier, U. Pfister for the COSY-Team,  
Forschungszentrum Jülich (KFA) GmbH, Postfach 1913, 5170 Jülich, Germany

### ABSTRACT

At present the cooler synchrotron COSY a synchrotron and storage ring for medium high energy physics is being built at Jülich. The cooler ring will deliver protons in the momentum range from 270 to 3300 MeV/c and has the option to accelerate  ${}^3\text{He}^{2+}$ ,  ${}^{12}\text{C}^{6+}$ ,  ${}^{16}\text{O}^{8+}$  and  ${}^{20}\text{N}^{10+}$  ions. The maximal number of stored protons will be  $2 \cdot 10^{11}$ . The phase space density of the circulating protons will be increased with electron cooling between the injection level and 600 MeV/c. The stochastic cooling system is designed to cool protons in the momentum range between 1500 and 3300 MeV/c. For external experiments averaged intensities up to  $\approx 2 \cdot 10^8$  cooled protons per second are expected with a duty cycle of  $\approx 50\%$  on quite narrow target spots. High luminosities can be achieved with solid targets in the internal beam.

The lattice parameters to match the different ion optical requirements for electron and stochastic cooling, acceleration, internal experiments and slow extraction are discussed. An overview of the ion sources, the injector cyclotron, the injection and extraction beamlines is given. Field measurements on the dipol and quadrupol magnets are reported. The results of the commissioning of the power converters and of the accelerating cavity are shown. The results on the sensitivity measurements of the beam position monitors are explained.

### 1. INTRODUCTION

The COSY facility consists of different ion sources, the cyclotron JULIC as injector, the injection beamline with a length of 100 m, the ring with a circumference of 184 m and the extraction beamlines to the external experimental areas. The high resolution beamline to the magnetic spectrometer BIG KARL, the beamline to the Time of Flight spectrometer (TOF) and the beamline for medical therapy application<sup>1)</sup> are under construction. In a later stage a fourth beamline will be added for polarization measurements. The layout of the COSY facility is shown in Fig. 1.

The lattice of the COSY ring consists of two 52 m long  $180^\circ$  bending sections, which are separated by two 40 m long straight sections. The straights are designed as telescopic systems with a 1:1 image from the beginning to the end with a phase advance either  $\pi$  or  $2\pi$ . Bridged by four optical triplets one straight section is dedicated to two internal target places TP 1 and TP2. The opposite straight section provides free space for the rf cavity, the electron cooler<sup>2)</sup>, scrapers, Schottky pick-ups and current monitors.

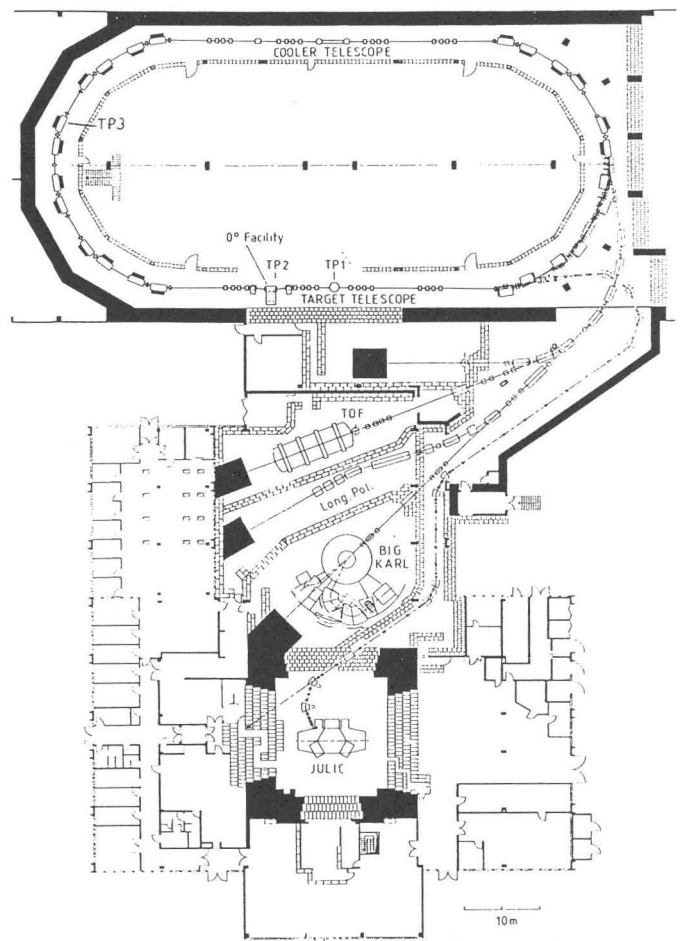


Fig. 1. Layout of the COSY facility.

The two arcs are composed of six mechanically identical periods. Each of the mirror symmetric half cells is given a QF-bend-QD-bend structure leading

to a six-fold symmetry of the total magnetic lattice. By interchanging the focussing and defocussing properties additional flexibility for adjusting the tune is achieved.

One of the bending arcs houses the injection and extraction devices, the stripping target, the magnet septum and bumper magnets for injection as well as the electrostatic and magnetic septa for extraction. The other arc offers space for a third internal target area TP3, which will make use of one of the ring magnets to separate  $0^0$  ejectiles, the diagnostic kicker and the elements for the ultra-slow extraction. At the intersection between straight sections and arcs the stochastic cooling pick-ups and kickers<sup>3)</sup> will be installed. The basic machine parameters are summarized in Table 1.

Table I  
COSY Basic Parameters

Vacuum system	
pressure in the arcs	$10^{-10}$ - $10^{-11}$ mbar
pressure in the straights	rectangular 150·60 mm <sup>2</sup> circular, $\phi$ 150 mm
RF system	
cavity type/ acceleration structure	symmetric re-entrant ferrite loaded
frequency range (h=1)	0.462-1.572 MHz
quality factor (at frequency)	8(400 kHz), 40(2 MHz)
max. rate of frequency increase	4 MHz/s
gap voltage (at duty cycle)	5 kV (100%), 8 kV (50%)
gap voltage dynamic range	55 dB
nominal/actual rf power	56/16 kW in push-pull
bending magnets	
number	24
radius	7 m
angle	15°
field range	0.23-1.585 T
quadrupole magnets in the arcs	
number	24
no. of families	6
eff. length	0.3 m
aperture radius	85 mm
max. gradient	7.5 T/m
quadrupole magnets in the telescopes	
number	32
no. of families	8
eff. length	0.55 m
aperture radius	85 mm
max. gradient	7.5 T/m
sextupole magnets	
number	18
no. of families	7
eff. length	0.3/0.2/0.1 m
aperture radius	85 mm
max. strength	30 T/m <sup>2</sup>

The magnetic lattice of the ring has to match different ion optical conditions:

- (i) the internal targets require low betatron functions and low dispersion
- (ii) the slow extraction needs the horizontal tune near a third order resonance
- (iii) the stochastic cooling demands a phase advance close to  $(2n+1) \cdot \pi/2$  between the pick-up and kicker location for both planes
- (iv) the electron cooler prefers low betatron amplitudes

These requirements can be fulfilled with the chosen working point. The beam and optical properties are listed in Table 2.

Table II  
Beam and Optical Properties of COSY

momentum range	270-3300 MeV/c			
max. no. of stored protons	$2 \cdot 10^{11}$			
horizontal/vertical tune	3.38/3.38			
transition momentum	1860 MeV/c			
geometrical acceptance	horizontal:	130 $\pi$ mm mrad		
	vertical:	35 $\pi$ mm mrad		
	$\Delta p/p$ :	$\pm 0.5\%$		
nat. chromaticity hor./vert.	- 5.2/- 4.5			
lattice function at				
	$\beta_{hor}$	$\beta_{vert}$	dispersion	
TP1:	5.6 m	5.9 m	0 m	
TP2:	1.6 m	5.1 m	0 m	
TP3:	6.0 m	22.2 m	10.1 m	
radii and divergences for an extracted emittance of $2.5 \pi$ mm mrad and $\Delta p/p$ of $1 \cdot 10^{-3}$ at				
	x/mm	x'/mrad	z/mm	z'/mrad
medical therapy area	3.25	1.34	1.88	1.24
Time of Flight	0.56	4.90	0.72	3.47
BIG KARL	0.45	7.14	0.43	6.92

## 2. ACCELERATOR COMPONENTS

### 2.1. Field Measurements of the Bending and the Quadrupole Magnets

The measurements of the bending magnets were done with sets of long coils, covering the whole beam field region. Seen in beam direction there are a long coil, two short coils located in the homogeneous part of the field and a second long coil. The coils are imbedded in a rod made from carbon fibre to be mechanically rigid. This coil support is driven across aperture of the magnet. Voltage induced in the coils are integrated. The reproducibility of the  $\int Bdl$  measurement is in the order of  $10^{-5}$ .

Figure 2 shows after shimming the relative deviation of  $\int Bdl$  of the individual magnets from the mean value of  $\int Bdl$  of all dipole magnets. The identity of the individual 24 dipole magnets is better than  $2 \cdot 10^{-4}$ .

The field components of the quadrupole magnets are determined on a measuring bench with slowly rotating coils. The quadrupole as well as the dipole component are compensated by a bucking coil, with

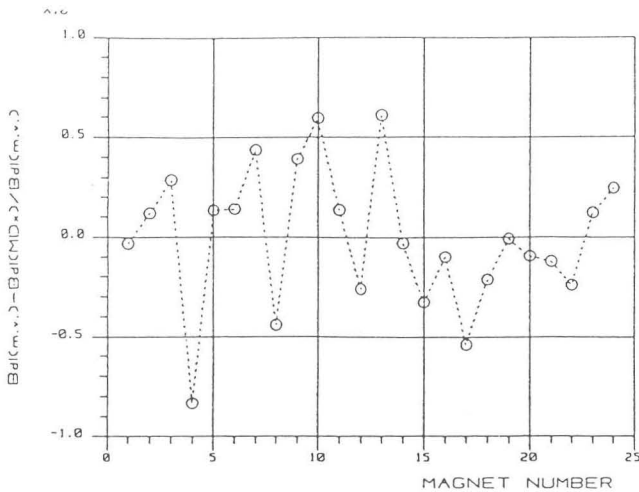


Fig. 2. Relative deviation of  $\int Bdl$  of the individual dipole magnets with respect to the mean value of  $\int Bdl$  of all the dipole magnets.

maximum sensitivity for harmonics  $n \geq 3$ . The achieved suppression of the quadrupole term was  $\sim 10^{-3}$ . The measuring probe consists of 3 sets of compensated coils. One long set integrates over the whole length of the magnets, the other two are integrating at the entrance and the exit sides of the quadrupole from inside the magnet to the field free region. After aligning the quadrupole on the measuring bench the excitation curve, the harmonic content as well as the gradient are measured for a number of currents. The gradient is deduced from the difference between the long coil and the two short coils. The relative deviation of  $\int gdl$  of the individual quadrupole magnet with respect to the mean values of  $\int gdl$  of all quadrupole magnets is shown in Fig. 3. Besides the quadrupole No. 1 which is the prototyp, the identity is better than  $4 \cdot 10^{-3}$ .

### 2.2. Power Converter

Only one power converter feeds 25 dipole magnets connected in series via a busbar system. Due to iron saturation the inductance decreases at max. current of 5000 A from 300 mH to about 100 mH. The load is changing its characteristic from a power consuming to a generating device at a current value of about 2600 A. This requires for proper operation two set values, the current set value and the set value for the output voltage. Figure 4 shows the actual current during ramping of the dipole magnet together with the difference signal of the actual current and the demanded current. During the ramping of the dipole the relative accuracy is better than  $2 \cdot 10^{-5}$ .

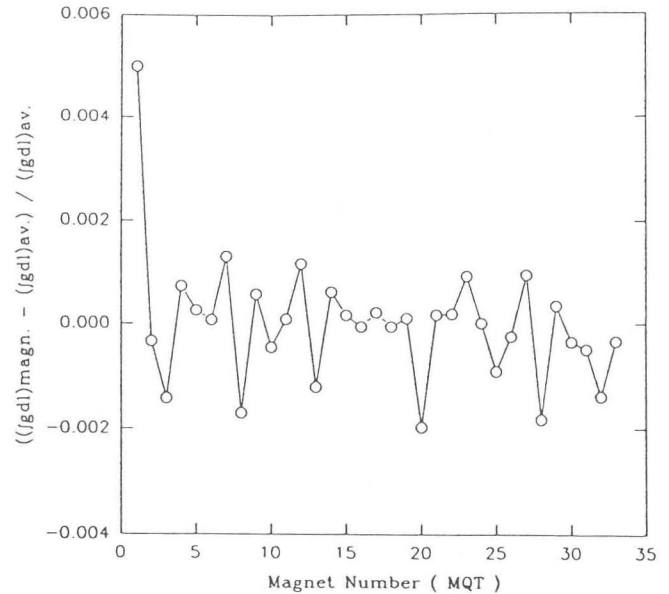


Fig. 3. Relative deviation of  $\int gdl$  of the individual quadrupole magnets MQT with respect to the mean value of  $\int gdl$  of all the quadrupole magnets MQT.

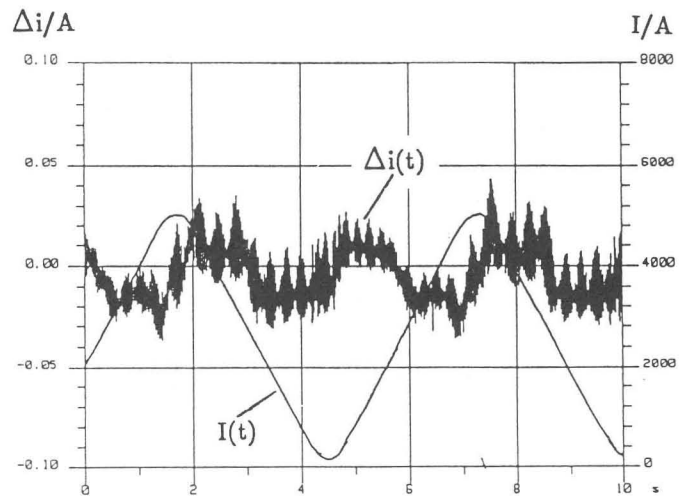


Fig. 4. Actual current  $I(t)$  during ramping and the differences  $\Delta i(t)$  of the actual current and the demanded current over the time  $t$ .

### 2.3. Accelerator System H = 1

The 50 kW rf acceleration system based on a ferrite-loaded coaxial cavity, has been developed in close cooperation with the Laboratoire National SATURNE and Thomson Tubes Electroniques. The accelerating system has been installed after measuring the rf properties with the extremely agile rf signal synthesizer for the control of the low level acceleration

signals. With this synthesizer the rf phase can be changed instantaneously. This rapid change of the acceleration phase of about  $180^\circ$  is necessary to pass through  $\gamma$  transition. Figure 5 shows the waveforms of the amplifier input and the resulting gap voltage during the phase switching procedure. The quality factor  $Q$  can directly be determined from the time of zero crossing of the envelope of the gap voltage. The relatively high  $Q$  factor of about 38 allows the realisation of a rapid phase switch.

DSA 602A DIGITIZING SIGNAL ANALYZER  
date: 11-DEC-91 time: 16:13:36

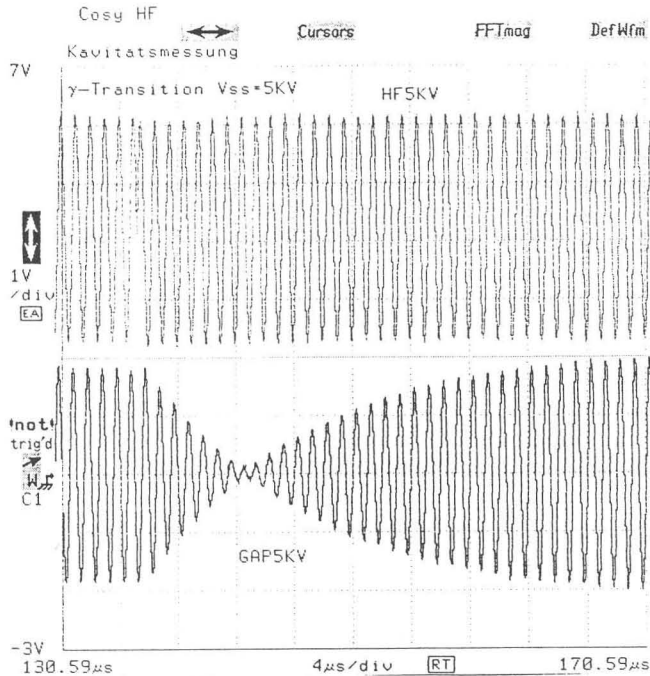


Fig. 5 The waveforms of the amplifier input and the resulting gap voltage during the phase switching procedure.

#### 2.4. Beam Position Monitors

For measurement of the transverse sensitivity of the beam position monitors (BPM) a test bench was installed. A 2 MHz-signal was injected to simulate the bunch current. The quantity difference  $\Delta(x)$  over the sum  $\Sigma$  of the electrode signals was measured in dependence of the position  $x$ . A linear dependence holds almost over the total BPM-aperture. This leads to a position sensitivity of  $10^{-2} \text{ mm}^{-1}$  in both planes of the cylindrical BPM. This value is in good agreement with the theoretical predictions. The position sensitivities of the rectangular BPM are  $7.5 \cdot 10^{-3}$  and  $2 \cdot 10^{-2} \text{ mm}^{-1}$  in the horizontal and vertical plane, respectively. The amplitude sensitivity or transfer impedance of the cylindrical BPM was measured in a  $50 \Omega$  matched coaxial system.

The set up allows to inject a well defined signal for beam current simulation in a large frequency range. In the case of high impedances ( $\geq 500 \text{ k}\Omega$  input impedance of the BPM preamplifiers) the transfer response is nearly constant in the frequency range 0.01-100 MHz. The transfer impedance of one electrode results to about  $3 \Omega$  in this frequency range. This agrees with the theoretical values for the transfer impedance of a particle, which moves with the speed of light.

### 3. SUMMARY

All magnetic elements for the ring, injection and extraction beam line have been installed in the final position. Measurements on stability, dynamic behaviour of the power converters with the final set ups of the magnetic elements are being completed. The commissioning of the injector cyclotron and parts of the injection beam line together with careful radiation protection measurement have been finished. The upgrade of the high resolution spectrograph BIG KARL is in progress. First injection into the cooler synchrotron and the commissioning are scheduled to start in autumn 1992. Start of users operation is aimed at April 1993.

### 4. ACKNOWLEDGEMENT

We would like to express our sincere thanks to our colleagues from accelerator laboratories around the world. We are indebted to the members of the machine advisory committee for their advice. We are grateful to the CANU members for stimulating discussions.

### 5. REFERENCES

- 1) Linz, U. and Maier, R., "A First Concept to Use the Cooler Synchrotron COSY-Jülich for Cancer Therapy," European Particle Accelerator Conference (EPAC), Berlin, March 1992.
- 2) Derissen, W., Maier, R., Pfister, U., Prasuhn, D., Sauer, M., Schwab, W., Schwarz, U., Sedlacek, M., Stein, H.J., Wimmer, J., Witt, J.D., and Zumloh, A., "Status of the COSY Electron Cooler," European Particle Accelerator Conference (EPAC), Berlin, March 1992.
- 3) Brittner, P., Hacker, H.U., Maier, R., Pfister, U., Prasuhn, D., Schug, G., Singer, H., Spieß, W., Stassen, R., Stockhorst, H. and Zumloh, A., "The Stochastic-Cooling System of COSY," European Particle Accelerator Conference (EPAC), Berlin, March 1992.